Long-term histologic and immunohistochemic findings in human venous aorto-coronary bypass grafts

Flavio Ribichini, Francesco Pugno, Valeria Ferrero, William Wijns, Giovanni Vacca, Corrado Vassanelli, Renu Virmani

Long-Term Histologic and Immunohistochemic Findings in Human Venous Aorto-Coronary Bypass Grafts.

Flavio Ribichini [*], Francesco Pugno[†], Valeria Ferrero[*], William Wijns[‡], Giovanni Vacca[§], Corrado Vassanelli[*], and Renu Virmani[‖].

Short title: Histopatholgy of saphenous vein grafts

Key words: atherosclerosis, pathology, saphenous vein graft, angioplasty, stents.

Division of Cardiology and Department of Biomedical Sciences and Surgery, University of Verona, Italy[*]. Laboratory of Human Pathology, Ospedale Cottolengo, Torino, Italy[†]. Cardiovascular Center of the OLV Hospital, Aalst, Belgium[‡]. Department of Clinical and Experimental Medicine, Università del Piemonte Orientale, Novara, Italy[§], CVPath, International Registry of Pathology, Gaithersburg, USA.

Address for correspondence:
Prof. Flavio Ribichini, MD
Director Catheterisation Laboratory
University of Verona
Ospedale Civile Maggiore-Borgo Trento
Piazzale Stefani 1, 37126 Verona, Italy.
Phone: +39 045 812 2039
Fax: +39 045 914 727
E-mail: flavio.ribichini@univr.it

Word count: 4801

The authors have no conflict of interest to report and the work did not receive financial support.

Abstract

Aim of the study was to analyse the long-term histology and immunohistochemistry of the plaque composition and cellular infiltration of saphenous vein grafts (SVG) containing metallic stents.

Percutaneous interventions in SVG bear a worse long-term clinical outcome compared to stenting of coronary arteries. Whether the pathologic features of old, degenerated SVG condition the efficacy of drug-eluting stents also is unknown.

Histology and immunohistochemistry of 7 SVG to the coronary circulation containing 12 metallic stents implanted 5 to 61 months before retrieval were analised in patients undergoing a second aorto-coronary bypass surgery at a mean time of 11±6 years.

Pathology of old SVG showed important thrombotic and necrotic composition of the plaque with plaque protrusion through the stent wires and a fragile media layer that can be easily damaged by stent placement with subsequent neointimal proliferation; indeed, stents showing medial fracture showed significantly greater mean neointimal thickness ($1.37\pm0.68mm^2$ versus $0.81\pm0.47mm^2$, $p<0.02$). Neointimal inflammatory cell density correlated with increased neointimal thickness in patent vessels ($r^2=0.43$, $p<0.001$). Immunostaining showed the total absence of estrogen receptors, a poor cellular proliferative state according to the presence of Ki-67 marker, persistent inflammation close to the stent wires marked by KP-1, and angiotensin-converting enzyme (ACE) immunostaining in most inflammatory cells in contact with the metal.

These pathologic findings may contribute to the more severe progression of disease and worse clinical outcome observed after conventional stented angioplasty of SVG and might also interfere with the efficacy of drug-eluting stents in this specific atherosclerotic milieu.

Abbreviations

ACE: angiotensin1-converting enzyme

DES: drug-eluting stent

ER: estrogen receptors

HPF: high power fields

SMC: smooth muscle cells

SVG: saphenous vein grafts

Introduction.

The implantation of endovascular stents in saphenous vein grafts (SVG) used as bypass conduits to revascularise the native coronary circulation is common practice in interventional cardiology. The percutaneous treatment of narrowed veins offers an excellent alternative to a second operation that in many cases can be avoided or at least delayed. Indeed, repeat bypass surgery is generally burdened by technical difficulties, older age, and a higher rate of graft occlusion [1].

Recent advances in stent technology and anti-platelet therapy, and the development of aspiration and protective devices to avoid distal embolisation during the procedure have improved the safety and short-mid term results of the transcatheter treatment of SVG [2]. Nevertheless, the progressive atherosclerotic degeneration of the venous conduit and the high rate of restenosis observed after stented angioplasty in this setting reduce the long-term efficacy of this approach that is burdened by a 40% rate of vessel failure compared to 15 to 20% in native coronary arteries [3].

The pathologic analysis of SVG treated with coronary stents is performed from surgical or autopsy specimens which are not easily available. Indeed, studies in this field are scarce and the description of pathologic changes of stented grafts available from previous reports is limited to relatively short periods. Previous studies performed in human venous bypass grafts have described the morphologic characteristics of restenosis after implantation of two different stent types [4-6]; other two studies have analysed the composition of in-stent restenotic plaques retrieved by means of directional atherectomy [7-8].

In the present study we analyse a series of SVG 11±6 years old (range 5-18 years) containing metallic stents that had been in place for as much as 5 years (range 5-61 months). The histology and the immunohistochemistry of the plaque composition and the cellular infiltration around the metallic stents are described.

The report is focused on the description of the salient features observed in this specific and rare histopathologic setting. Such information may be of help to evaluate possible differences of efficacy between drug-eluting stents (DES) and conventional metallic stents implanted in degenerated SVG.

Methods

Our study describes the pathology of 7 SVG containing 12 coronary stents, retrieved from 6 patients (table 1). All patients gave their informed consent to the analysis of the surgical specimens and angiographic images, and the approval of the Ethical Committee of the institution where the study material was analysed (Ospedale Maggiore di Novara, Italy) was obtained.

All patients were treated with balloon dilatation and/or stent implantation because of recurrence of angina secondary to the stenosis of one graft. At a mean time of 11±6 years the patients were re-operated because of recurrent angina secondary to the angiographic documentation of a total occlusion of the graft in 3 cases, and to stent restenosis and or progression of the disease in other grafts in the remaining patients. At the time of the repeat surgical intervention the stented grafts were harvested, rinsed with saline an fixed in 9% neutral buffered formalin. The proximal edge of the graft was marked with a suture stitch to identify the anatomic orientation and allow comparison with the angiographic images.

Pathologic examination.

Using the suture stitch as a landmark, the localisation of the stents within the SVG was assessed by a radiographic examination that allows the precise identification of each stent length, the detection of overlapped or under-expanded segments and the comparison with the last digital angiographic image of the graft before surgical retrieval. The SVG segments were placed into processing vials and dehydrated in a graded series of alcohols. Samples were then infiltrated with methylmethacrylate plastic and placed in airtight vials in a 39°C waterbath for polymerisation. Afterwards, blocks were cut at 2-3mm intervals along the stented and non stented vein segments. Plastic sections (4-6µm thick) were then cut, adhered to glass and allowed to dry. The plastic was then removed, and the sections selected for analysis (nearly 100 per segment) were rehydrated and stained. In segments selected for immunohistochemistry the stent wires were carefully removed under a dissecting microscope taking care not to alter the macroscopic wall structure before paraffin embedding. Plastic and paraffin sections were stained with hematoxylin and eosin and Movat pentachrome. The SVG segments showing different degrees of lumen stenoses were selected for analysis i.e, total occlusion, severe, moderate or mild stenosis of the vein that correspond to diameter stenosis 100%, <100≥50%, <50≥30% or <30 respectively, and cross-sectional area stenosis of 100%, >75%, 75-50% and <50% respectively. The following area measurements were made on each section: stent area, underlying plaque, lipid cores, calcified cores, vessel lumen, and in-stent neointima. Fibrocellular tissue was graded as *paucicellular or fibrotic* [<30 spindled cells in high power fields (HPF)], *moderately cellular* (30-100 spindled cells HPF) and *hypercellular* (>100 spindled cells HPF). Sections were further magnified (x200) and 4 fields containing stent struts (12, 3,6 and 9 o'clock) were selected for analysis of neointimal details [neointimal thickness (mm) and area (mm^2), neovessels and inflammatory cell density around the stent struts in terms of cells/mm^2 that was classified as being *slight:* 1-10 inflammatory cells/struts, *moderate:* 11 to 20 cells/struts, or *severe:* >20 cells/struts]. The stent strut penetration was categorised as being associated with

the fibrous plaque (or an intact fibrous cap or intact media), medial injury, or lipid core or atheroma penetration [9].

Immunohistochemistry.

Immunostaining for the detection of smooth muscle cells (SMC), macrophages, cells containing angiotensin1-converting enzyme (ACE), proliferation marker Ki-67 and estrogen receptors (ER), were performed in selected samples of non-stented and stented segments of all veins using previously described techniques [10].

Cellular ACE activity was investigated because ACE has been observed in the atherosclerotic plaque as a mediator of inflammation and in the process of wound healing after percutaneous injury of the vessel wall, and to identify endothelial cells [11-12]. Estrogenic activity was investigated because of the protective mechanisms exerted by estrogenes in the vascular wall [13-15]. The total vessel area of positively stained segments for each immunologic reaction was quantified by computer-aided planimetry of each specimen using an acquisition program Image Pro Plus (Media Cybernetics, software version 4.0, Silver Spring, MD, USA) in order to determine a percentage of tissue surface containing different cellular types.

Statistical analysis.

Continuous data are expressed as means and standard deviations; discrete variables are given as absolute values and percentages. Two-tailed Student's t test was used for comparison of parametric variables and the chi-square or exact test for discrete variables. A linear regression analysis was used to correlate the number of inflammatory cells around the stent struts and neointimal thickness. A probability value <5% was considered significant.

Results.

Histology.

Patients clinical characteristics, procedural details of stent implantation, timing and the reason for surgical re-intervention are shown in Table 1.

The angiographic examination obtained before repeat bypass surgery showed 3 totally occluded SVG (each one containing one, two and three stents respectively, and variable degrees of neointimal growth within the stents). In the remaining cases, a mild stenosis within the stent was analysed in 3 stents in 3 different patients and a moderate-severe stenosis in other 3 stents implanted in 3 different patients. Segments of SVG with mild, moderate and severe stenosis not covered by the stents were also analysed.

Stents showing medial fracture were associated with a significantly greater mean neointimal thickness ($1.37\pm0.68mm^2$ versus $0.81\pm0.47mm^2$, $p<0.02$). In one case, the stent struts of two sequential stents were partially apposed to a large aneurysm, leaving a space between the struts and the SVG wall filled with thrombus, and atheroma (Figure 1a and 1b). The degree of stent wall indentation, the luminal SVG %

diameter stenosis and area narrowing, as well as the main histologic characteristics, are reported in Table 2, that briefly describes the classification scheme proposed by Virmani et al [16].

Histology of the stented SVG segments: in totally occluded SVG, red thrombus was observed in all cases as well as large amount of organised thrombus containing neovessels (Figure 2). The presence of neovessels has been well described in native coronary arteries with total occlusion [17]. In 2 of the 3 totally occluded cases a stenosis of the graft was present proximally to the stented segment and in one case the stenotic plaque was in the mid portion of the under-expanded stent, two mechanisms previously related to SVG stent occlusion [6]. Histology of the underlying stenotic lesions showed predominance of smooth muscle cells that extended from the metallic wires towards the vessel lumen within an extensive extracellular proteoglycan/collagen matrix (Figure 2). The lumen side of the stent showed a slight to moderate degree of inflammation (i.e. >1 to <20 cells adjacent to each stent strut), and giants cells were frequently observed. The vessel wall showed a thin smooth muscular layer of the vein media (average 900±300μm) and of the collagenous adventitia (average 650±400μm**)**. When the stent struts caused laceration or rupture of the vein medial wall, a thickened adventitia **(**>1mm) was observed in correspondence of a thickened neointima toward the luminal side. Large calcium deposits (range 2 to 8.7mm^2) were observed in all cases, always surrounded by inflammatory infiltrate of histiocytes and lymphocytes.

In patent stents, plaques causing different degrees of luminal stenoses were characterised by a similar histologic pattern, mainly composed by SMC and extracellular matrix. A moderate to severe infiltration of inflammatory cells (10-20 or >20 cells/strut) was observed when the stent strut was adjacent to injured media or a lipid core rather than a fibrous plaque, confirming in the veins a mechanism previously described in native coronary arteries [9]. Furthermore, when the stent struts were in contact with an underlying plaque mainly composed of a necrotic core, no healing was present (Figure 3a) and plaque and thrombus protruding into the vein lumen were observed (Figure 3b). Different degrees of inflammation around the stent struts correlated with neointimal thickness in patent vessels, indeed, by linear regression analysis, a significant correlation was found between the areas occupied by inflammatory cells and the intimal thickness around the stent struts of plaques analysed in patent conduits (r^2=0.43, $p<0.001$).

The degree of penetration in the vessel wall was not different for self-expanding or balloon expanding stents. This may correspond to aggressive post-stent high-pressure balloon dilatation or to the injury caused by the self-expanding stent type that exerts a permanent radial force on the vessel wall. An interesting pathologic feature of plaques causing only a mild narrowing of the vein lumen is the presence of a circular layer of calcium around the stent. In these cases, organised thrombus was rarely observed and neointimal growth was only mild (Figure 4).

Histology of the non-stented SVG segments: vein plaques were fibrous with calcified areas and chronic inflammatory infiltrates. Stenoses causing SVG lumen narrowing were mainly composed of organised thrombus with neovessels. Histiocytes and less frequently lymphocytes were observed beneath the endothelial layer that covers the intima. In the lumen of the SVG, red thrombus was observed in as many of 70% of analysed segments (Figure 5).

Restenotic or primary lesions: primary lesions were composed mostly by moderately cellular plaques (30-100 spindled cells HPF) while restenotic plaques showed a trend to be predominantly paucicellular (<30 spindled cells/HPF). No significant differences in extracellular matrix formation or cell proliferation were observed between primary and restenotic SVG tissue, in contrast to previously described findings in arterial tissue [18]. The lack of a diagnostic pattern that differentiate primary from restenotic plaques in SVG has been reported previously by other authors [5,8].

Stents in place for less than 6 months: pathology of stent analysed within 6 months of implantation revealed moderate-severe inflammation of the media around the stent wires (10-20 or >20 cells/strut respectively), neointimal proliferation and SMC; the endothelial layer was not always observed and when present, the endothelial cells showed large nuclei and polygonal cellular shape.

Stents in place from 6 months to 2 years: neoendothelium showed a thin layer of cells with a normal aspect covering the neointima located within the stented segments. Large calcified semicircular areas with moderate inflammation near the calcified core and the metallic wires were observed. In some areas, macrophages included iron pigments.

Stents in place from 2 to 5 years: appeared basically as described above, with more intense infiltration of lymphocytes under the endothelial layer, and giant cells close to the stent struts. Calcified areas of the vessel wall were larger the older the SVG (mean calcified surface in veins >10 years 6.8±3.4mm^2 versus 3.4±3.0mm^2 in veins ≤10 years, $p<0.01$).

Immunohistochemistry

Immunostaining for *alpha actin* identified SMC's as the cellular component of 40 to 80% of the media layer in all cases, and rare elements in the adventitia. In the lumen side, cellular components of the neointima within the stent revealed SMC's accounting for 55% of the neointimal area, and a rich extracellular fibrous matrix. There were more SMC's close to the neoendothelium than close to the stent struts (53% versus 12%, $p<0.01$), but the percentage area of stained cells did not differ among the different types of tissue analysed (Table 3).

KP-1 staining was observed in areas of cluster of macrophages in all cases. In the underlying plaque KP-1 stained macrophages situated close to the necrotic or the calcified cores and the external side of the metallic stent struts. Some inflammatory cells were also observed in the adventitia. In the neointima, KP-1 positive cells were in contact with the metallic struts (Figure 6a), and beneath the neo-endothelial layers when this was present. In plaques causing severe in-stent restenosis KP-1 positive cells were significantly more frequent than in plaques causing only mild in-stent stenosis (Table 3). In non-stented segments KP-1 stained cells were also present close to necrotic, atheromatous or calcified cores.

ACE activity was detected mostly in cells that co-localised for KP-1 in identical sections, suggesting their inflammatory nature. These cells were most commonly observed close to the stent wires (Figure 6b), and in some cases close to the adventita. A second type of ACE positive cells that did not stain for KP-1 were identified as endothelial cells of neovessels of the plaque and cells of the neo-endothelium that faced the vessel lumen. A third group of ACE positive cells that co-localised for alpha actin in identical sections was

observed in the media and the sub-endothelial layer of the neointima with a spindle-shape morphology. In plaques causing in-stent restenosis there was significantly more ACE activity in macrophages compared with plaques of non-stented vein segments (Table 3).

Immunostaining for Ki-67 showed few positive cells, suggesting the poor proliferative state of the old veins. There was no difference as to the amount of Ki-67 positive cells between restenotic or "de-novo" lesions and between plaques causing severe or mild in-stent obstructions (Table 3).

Immunostaining for ER was completely negative in all the sections examined irrespective of the patient's gender and of the presence of a stent.

Discussion

Despite the improvement of the immediate results of transcatheter treatment of diseased SVG [2], the long-term outcomes remain sub-optimal [3]. The reasons for such unfavorable results are probably related to the nature of the venous wall and the changes that follow the implantation of the vein in the systemic circulation [19]. Metallic stents may interact with the venous wall in a different manner compared to the arterial wall, the more fragile media layer and the friable atherosclerotic type of plaque of the SVG can be easily damaged by percutaneous devices inducing a subsequent exaggerated reparative response.

Our study extends the available knowledge about the long-term effects of metallic stents in SVG up to 5 years after implantation, and about the evolution of the atherosclerotic disease of the SVG wall up to 18 years. The main findings of our research can be summarised as follows.

1. Histology shows, on the one hand, that the media layer of the SVG, being thinner than that of coronary arteries, is likely more susceptible to the mechanical damage caused by the stents and the balloon pressure, and that the easier media fracture ensues aggressive neointimal proliferation. On the other hand, very long-term chronic inflammation close to the metallic wires is a relevant phenomenon, and similarly to what has also been reported in coronary arteries, this finding correlates with thicker neointima within the stents [9,20]. However, organised thrombus with neovessels represent the main component of the lumen-narrowing material (particularly in totally occluded conduits), while substantial amounts of plaque easily protrude into the SVG lumen after stent placement. The larger diameter and the lower elasticity of the vein conduit may cause a less brisk flow in the SVG that fosters platelet apposition, thrombus formation and subsequent lumen narrowing. Thus, the atherosclerotic material of SVG lesions appears highly friable because it lacks excess collagen and is richer in lipids, necrotic cores and macrophages facilitating plaque prolapse through the stent struts.

Unlike native coronary arteries, in which calcification is basically seen in the intima, embedded in the collagen matrix, and focally precipitated in necrotic cores, atherosclerosis of the degenerated SVG is characterized by large areas of calcification of the vessel wall itself. In particular, in segments of veins with only mild in-stent proliferation calcium deposition may assume a circular pattern embedded in a thin

muscular wall, and these annular calcified areas are more extensive the longer the time of the implant in the arterial circulation.

2. Immunohistochemic assays show a long-lasting presence of macrophages staining positively for KP-1 and ACE, confirming a preliminary report from our group in which ACE activity in cells close to the stent wires was observed after 6 months of stent implantation in an artery [21]. Such observation extends the concept proposed by Komatsu et al that demonstrated ACE activity as a mediator of inflammation but being limited to short time after balloon arterial wall injury [22]. This phenomenon was observed predominantly in sections of veins that received a coronary stent. The presence of ACE was not only referred to inflammatory cells; indeed, ACE immunostaining was observed in endothelial cells, as expected, but also in groups of neointimal spindle-shaped cells that stained also positively alpha actin. This finding suggests a possible role of the enzyme in the transformation of SMC-like cells from a dedifferentiated to a differentiated phenotypic state or from other type of cells such as infiltrating macrophages or fibroblasts as it has been previously proposed in native coronary arteries [10,12,22]. A predominant role of ACE in the repairing process of wall damage in SVG is supported by the threefold greater ACE activity observed in human SVG compared to the internal thoracic artery of patients re-operated 20 years after a first coronary bypass surgery [23].
Immunostaining for the detection of ER was totally negative in these samples. The absence of ER in the saphenous vein is in agreement with previous observations [24-25]; some rare ER may be found in veins of fertile women, but not in men or post-menopausal women [24]. The lack of the anti-atherosclerotic effects of estrogens in the structure of the vein wall may contribute another possible reason for the aggressive atherosclerotic degeneration of the veins used as by-pass grafts [15].
The rare presence of cells staining with the proliferation marker Ki-67, put in evidence the poor proliferative state of this type of tissue, and suggests that organised thrombus and migrated cells rather than cell proliferation could be the principal reasons of SVG lumen narrowing.

The recent availability of DES has dramatically improved the efficacy of percutaneous coronary interventions in native vessels but very scarce information is available regarding the efficacy of DES implanted in old degenerated SVG [26-28]. Furthermore, data about the histopathology of such kind of stents implanted in old SVG is not available so far. Commercially available DES inhibit restenosis on coronary arteries exerting mainly anti-blastic and anti-proliferative effects [29]; therefore, from a practical standpoint, DES may exert different levels of effectiveness (either higher or lower) in old, degenerated atherosclerotic SVG according to the predominant histopathologic characteristics observed in these plaques, as described in the present study.

References

1) Foster ED, Fisher LD, Kaiser GC, et al. (1984) Comparison of operative mortality for initial and repeat coronary artery bypass grafting: the Coronary Artery Surgical Study (CASS) Registry Experience. Ann Thorac Surg **38,**563-570
2) Baim D S, Wahr D, George B, et al on behalf of the SAFER Trial investigators. (2002) Randomized trial of a distal embolic protection device during percutaneous intervention of saphenous vein aorto-coronary bypass grafts. Circulation **105**,1285-1290
3) Choussat R, Black AJR, Bossi I, et al. (2000) Long-term clinical outcome after endoluminal reconstruction of diffusely degenerated saphenous vein grafts with less-shortening wallstents. J Am Coll Cardiol **36**,387-394
4) Anderson PG, Bajaj RK, Baxley WA, et al. (1992) Vascular pathology of balloon-expandable flexible coil stents in humans. J Am Coll Cardiol **19**,372-381
5) Van Beusekom HMM, van der Giessen WJ, van Suylen RJ, et al. (1993) Histology after stenting of human saphenous vein bypass grafts: observations from surgically excised grafts 3 to 320 days after stent implantation. J Am Coll Cardiol **21,**45-54
6) Depre C, Havaux X, Wijns W. (1998) Pathology of restenosis in saphenous bypass grafts after long term stent implantation. Am J Clin Pathol **110**,378-384
7) Strauss BH, Umans VA, van Suylen RJ, et al. (1992) Directional atherectomy for tretament of restenosis within coronary stents: clinical, angiographic and histologic results. J Am Coll Cardiol **20**,1465-1473
8) Nikol S, Huehns TY, Weir L, et al. (1998) Restenosis in human vein bypass grafts. Atherosclerosis **139,**31-39
9) Farb A, Sangiorgi G, Carter A, et al. (1999) Pathology of acute and chronic coronary stenting in humans. Circulation **99,**44-52
10) Ribichini F, Pugno F, Ferrero V, et al. (2006) Cellular immunostaining of angiotensin-converting enzyme in human coronary atherosclerotic plaques. J Am Coll Cardiol **47**,1143-1149
11) Diet P, Pratt RE, Berry GJ, et al. (1996) Increased accumulation of tissue ACE in human atherosclerotic coronary artery disease. Circulation **94**,2756-2767
12) Ohishi M, Ueda M, Rakugi H, et al. (1997) Upregulation of angiotensin-converting enzyme during the healing process after injury at the site of percutaneous transluminal coronary angioplasty in humans. Circulation **96**,3328-3337
13) Dai-Do D, Espinosa E, Liu G, et al. (1996) 17 beta-estradiol inhibits proliferation and migration of human vascular smooth muscle cells: similar effects in cells from postmenopausal females and in males. Cardiovasc Res **32**,980-985
14) Chandrasekar B, Nattel S, Tanguay JF. (2001) Coronary artery endothelial protection after local delivery of 17beta-estradiol during balloon angioplasty in a porcine model: a potential new pharmacologic approach to improve endothelial function. J Am Coll Cardiol **38**,1570-1576

15) Geraldes P, Sirois MG, Tanguay JF. (2003) Specific contribution of estrogen receptors on mitogen-activated protein kinase pathways and vascular cell activation. Circ Res **93**,399-405

16) Virmani R, Kolodgie FD, Burke AP, et al. (2000) Lessons from sudden coronary death. A comprehensive morphological classification scheme for atherosclerotic lesions. Arterioscler Thromb Vasc Biol **20,**1262-1275

17) Depre C, Havaux X, Wijns W. (1996) Neovascularization in human coronary atherosclerotic lesions. Cathet Cardiovasc Diagn **39**,215-220

18) Riessen R, Isner JM, Blessing E, et al. (1994) Regional differences in the distribution of the proteoglycans biglycan and decorin in the extracellular matrix of atherosclerotic and restenotic human coronary arteries. Am J Pathol **144**,962-974

19) Kalan JM, Roberts WC. (1987) Comparison of morphologic changes and luminal sizes of saphenous vein and internal mammary artery after simultaneous implantation for coronary arterial bypass grafting. Am J Cardiol **60**,193-196

20) Farb A, Weber DK, Kolodgie FD, et al. (2002) Morphological predictors of restenosis after coronary stenting in humans. Circulation **105**,2974-2980

21) Ribichini F, Pugno F, Ferrero V, et al. (2000) Angiotensin-converting enzyme tissue activity in the diffuse in-stent restenotic plaque. Circulation **101**,e33-e35

22) Komatsu R, Ueda M, Naruko T, et al. (1998) Neointimal tissue response at sites of coronary stenting in humans. Circulation **98**,224-233

23) Borland JA, Chester AH, Crabbe S, et al. (1998) Differential action of angiotensin II and activity of angiotensin-converting enzyme in human bypass grafts. J Thorac Cardiovasc Surg **116**,206-212

24) Bergqvist A, Bergqvist D, Ferno M. (1993) Estrogen and progesterone receptors in vessel walls. Biochemical and immunochemical asays. Acta Obstet Gynecol Scand **72**,10-16

25) Perrot-Applanat M. (1996) Estrogen receptors in the cardiovascular system. Steroids **61,**212-215

26) Ge L, Iakovou I, Sangiorgi GM, et al. (2005) Treatment of saphenous vein graft lesions with drug-eluting stents: immediate and midterm outcome. J Am Coll Cardiol **45**,989-994

27) Vermeersch P, Agostoni P, Verheye S, at al. (2006) Randomized double-blind comparison of sirolimus-eluting stent versus bare-metal stent implantation in diseased saphenous vein grafts: six-month angiographic, intravascular ultrasound, and clinical follow-up of the RRISC Trial. J Am Coll Cardiol **48,**2423-2431

28) Rocca HP, Kaiser C, Pfisterer M. (2007) Targeted stent use in clinical practice based on evidence from the Basel Stent Cost Effectiveness Trial (BASKET). Eur Heart J **28**,719-725

29) Costa M, Simon DI. (2005) Molecular basis of restenosis and drug-eluting stents. Circulation **111**,2257-2273

Figure Legends

Figure 1. (a): X-ray photography of a SVG containing 2 overlapped metallic stents at the site of a large aneurysm (arrow) and a third stent beyond. **(b):** hematoxylin-eosin cross-section of the same SVG (x2) showing the patent lumen of the stents and the aneurysm lumen filled with fresh thrombus (arrows).

Figure 2. Movat Pentachrome staining (x4) of a totally occluded SVG: the lumen of the conduit is occupied by a thick neointima within the stent and a totally occlusive organized thrombus (arrows).

Figure 3. (a): Cross-section of a SVG implanted a self-expanded metallic stent and developing late in-stent restenosis. The stent struts show deep apposition close to the media layer on the left side of the SVG section and a thick neointima developed within the stent lumen close to the struts (asterisk). The wires on the right side (arrow) are close to a necrotic core and only a thin layer of healing neointima is observed in the lumen side of the stent struts. (Movat Pentachrome section x2). **(b):** Atherosclerotic plaque and large thrombus protruding into the SVG lumen through the stent struts (asterisk). (Movat Pentachrome section x4)

Figure 4. Large circular calcification around the stent struts and mild neointimal growth at the luminal side of the stent (hematoxylin-eosin section x4).

Figure 5. Movat Pentachrome stained cross-section (x4) of a non-stented segment of SVG previously treated with balloon angioplasty and showing late luminal narrowing (asterisk), thickened neointima (1), organized thrombus (2), red thrombus (3) and neovessels of the thickened adventita (4) are evident.

Figure 6. (a): Immunohistochemistry staining showing brown-colored cells positive for human panmacrophagic antibody KP-1 close to the stent wires removed for paraffin embedding (asterisk). The KP-1 positive staining demonstrate the inflammatory nature of the cells around the metallic struts (x200). **(b):** ACE immunostaining showing positive reaction (brown-colored elements) in inflammatory cells close to the metallic strent wire removed for paraffin embedding (asterisk).

Table 1. Characteristics of 6 patients treated with 12 stents in 7 SVG.

Pt	Age	Sex	Type of graft	Type of stent	Previous PTCA	Stent diameter and length	Maximal pressure	Duration of implant (months)	Graft age (months)	Stent implant reason	SVG retrieval reason
1	64	M	SVG-RCA	Wallstent	Yes	4.5 x 30 mm	8 atm	6	64	SA CCS II	Total occlusion CCS : II
2	68	M	SVG-LAD	Wallstent	No	5.5 x 20 mm	12 atm	32	188	UA IB	Mild stenosis and acute total occlusion. PTCA before re-CABG
			SVG-RCA	Palmaz-Schatz	No	3.5 x 30 mm	16 atm	60	188	UA IB	CCS: III
			SVG-RCA	Wallstent	Yes	5 x 47 mm	20 atm	1	188		
			SVG-RCA	Wallstent	Yes	4.5 x 24 mm	20 atm	1	188		
3	67	M	SVG-RCA	Wallstent	No	4.5 x 31mm	6 atm	5	125	UA IIC	Progression of disease in other grafts CCS: III
4	74	F	SVG-LAD	Wallstent	Yes	3.5 x 34 mm	12 atm	7	50	UA III B	Restenosis and progression of disease
			SVG-LAD	Multilink	No	3.0 x 8 mm	13 atm				in other grafts CCS: IV
5	74	M	SVG-RCA	Wallstent	No	5.0 x 30 mm	10 atm	26	218	SA CCS III	Total occlusion
			SVG-RCA	Wallstent	No	4.0 x 30 mm	10 atm	26	218		CCS :III
6	77	F	SVG-OM	Wallstent	No	3.5 x 20 mm	10 atm	40	159	UA III B	Restenosis and progression of disease
			SVG-OM	Wallsent	No	3.5 x 13 mm	10 atm	40	159		in other grafts CCS: II

Abbreviations: M: male, F: female, SVG: saphenous vein graft, RCA: right coronary artery, LAD: left anterior descendent, OM: oblique marginal, PTCA: percutaneous transluminal coronary angioplasty, atm: atmosphere, SA: stable angina, UA: unstable angina, CCS: Canadian Cardiac Society.

Table 2. Main histologic findings.

Pt n	Angiographic result	Area luminal narrowing	Depth of injury	Main histologic observations and lesion's classification (16)
1	%DS= 100 %DS=33	100%	M*	***Type of lesion: Atherosclerotic plaque with rupture.*** **UP:** atrophia of media and adventitia, intense inflammation around the metallic struts. **NI:** organized thrombus and SMC with neo-vessels in the neointima.
2	%DS= 15	24%	FP	***Type of lesion: Fibrocalcific plaque.*** **UP:** Circular calcification with few inflammatory cells. **NI:** endothelial cells covering collagenous matrix around the wires, few inflammatory cells below the endothelium and thin neointima.
	Acute total occlusion recanasiled with emergency PTCA		FP/AP	***Type of lesion: Thin fibrous cap with necrotic core and hemorrhage.*** **UP:** large aneurysm containing organized thrombus, macrophages and cholesterol debries. Calcium and severe inflammation in atrophic media. **NI:** stent struts covered by a thin layer of thrombus and no endothelial cells.
3	%DS= 38	60%	FP/AP/M*	***Type of lesion: Plaque with rupture.*** **UP:** inflammation around the stent wires, giant cells. **NI:** neointimal growth of SMC and organized thrombus.
4	%DS= 16 %DS= 40	16% 40%	FP	***Type of lesion: Fibrocalcific plaque.*** **UP:** large calcification, inflammatory cells and giant cells around the stent wires. **NI:** red thrombus, macrophages infiltration under a thickened neointima, SMC.
5	%DS= 100 %DS= 55	100% 84%	FP M-EL*	***Type of lesion: Pathologic intimal thickening.*** **UP:** atrophia of the media and adventitia, rare SMC in a rich extracellular matrix. Inflammatory cells around the stent wires. **NI:** thick neointima of SMC causing severe stenosis with chronic inflammatory cells containing hemoglobin pigments
6	%DS= 28 %DS= 46	43% 72%	FP FP/M*	***Type of lesion: Fibrocalcific plaque.*** **UP:** SMC and chronic inflammatory cells. **NI:** endothelial cells and collagenous matrix, macrophages around the metallic wires, circular calcification with thin endothelium.

*Abbreviations: %DS: percent diameter stenosis, EL: elastic lamina, M: media, AP: atheromatous plaque, FP: fibrous plaque, NI: neo-intima, SMC: smooth-muscle cells, UN: underlying plaque. * asterisks denotes disrupted media.*

Table 3. Quantitative immunohistochemic analysis.

Type of SVG sample	alpha actin *	p value	KP1*	p value	ACE*	p value	Ki-67*	p value	ER
De novo lesion	58±35	NS	21±15	NS	18±16	NS	1	NS	-
Restenotic lesion	49±31		27±19		22±19		1		-
Severe in-stent restenotic lesion	51±31	NS	33±20	<0.05	25±24	<0.05	1	NS	-
Mild in-stent lesion	45±40		18±14		10±7		1		-
Stented SVG	54±33	NS	22±18	NS	19±17	<0.05	1	NS	-
Non stented SVG	56±27		16±12		9±6		1		-

Abbreviations: SVG: saphenous vein graft, ACE: angiotensin-converting enzyme. (*) indicates % of plaque area.

Figure 1

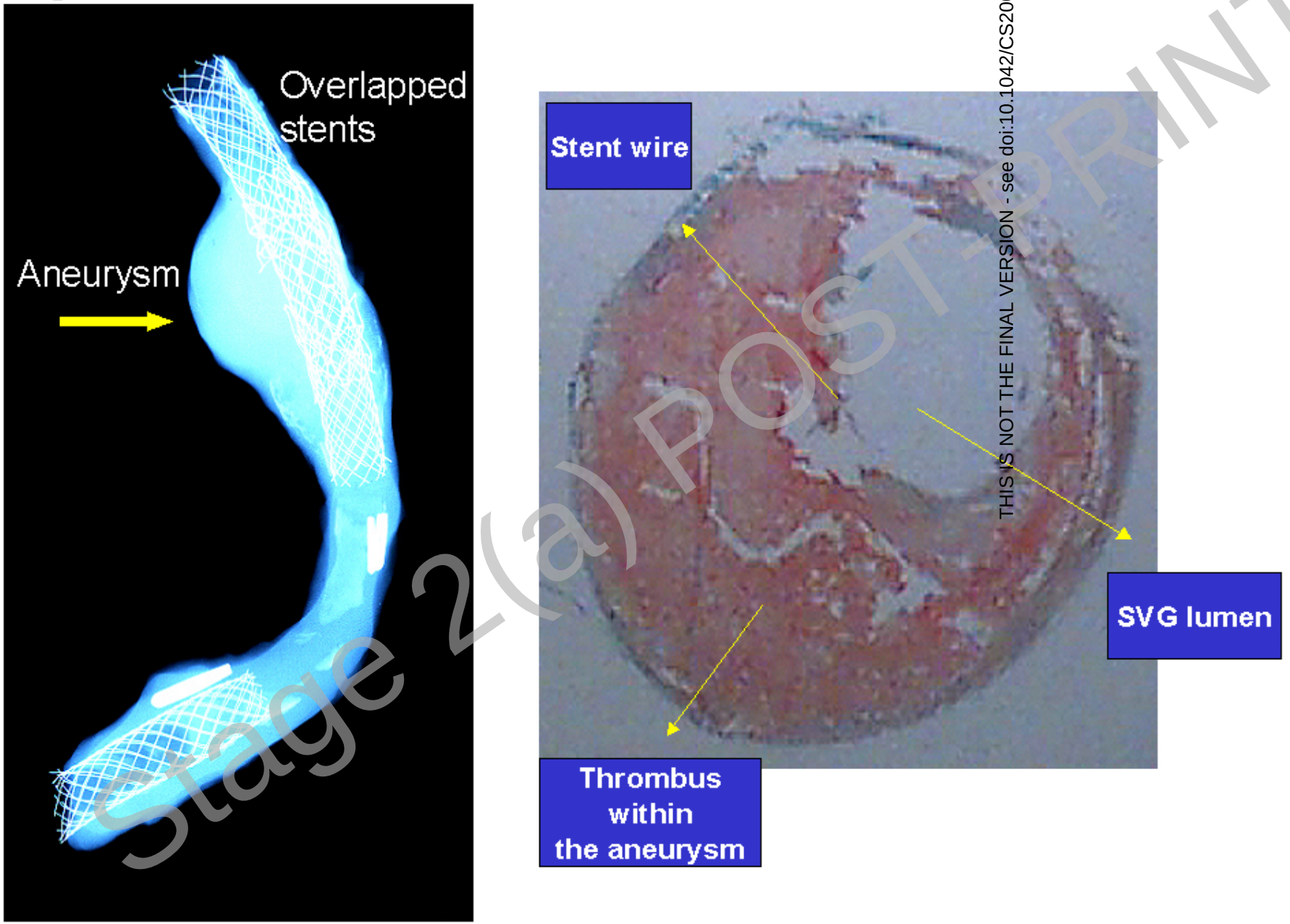

Figure 2

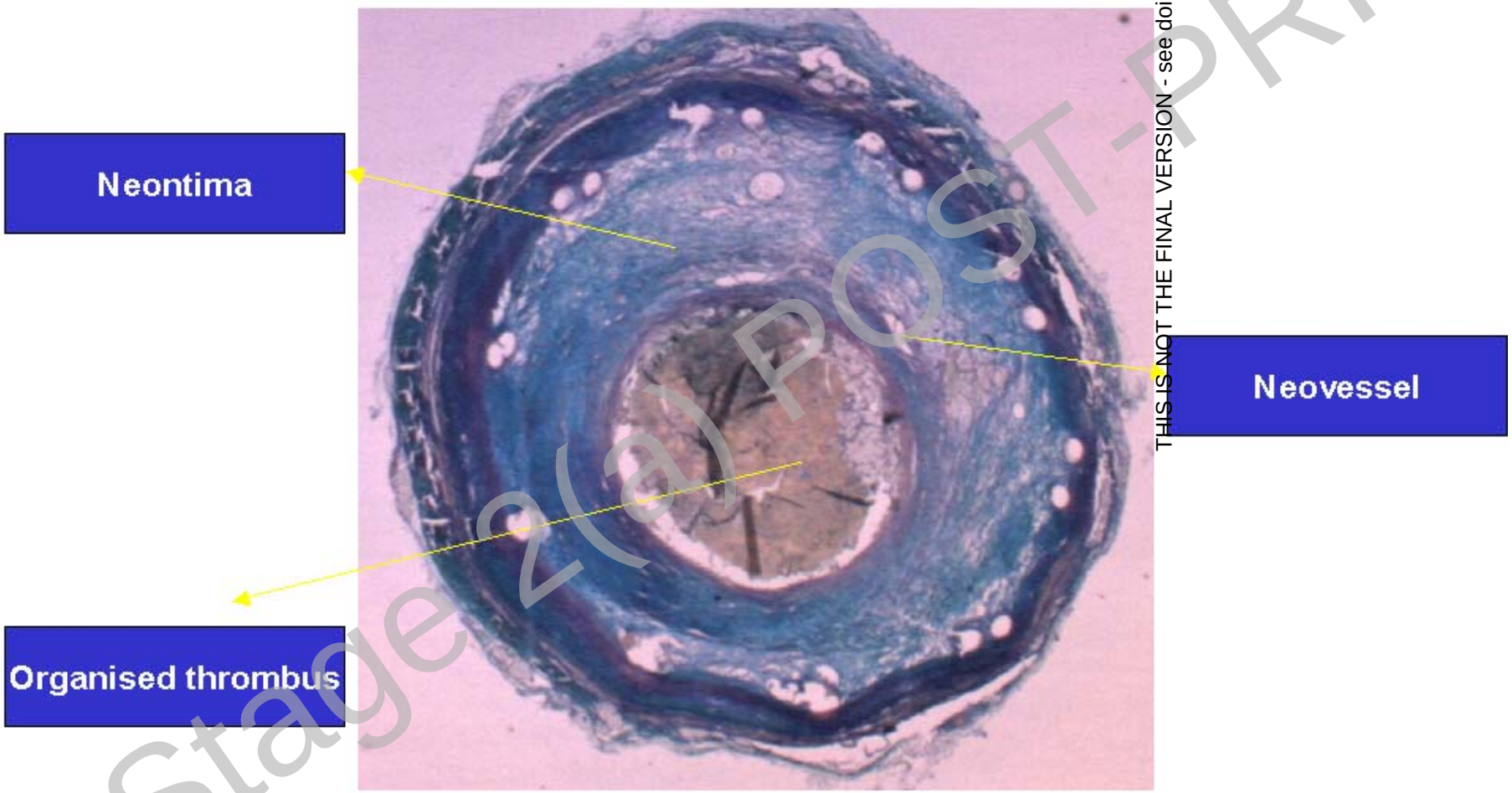

Clinical Science Immediate Publication. Published on 12 Sep 2007 as manuscript CS20070243

Figure 3

(a)

(b)

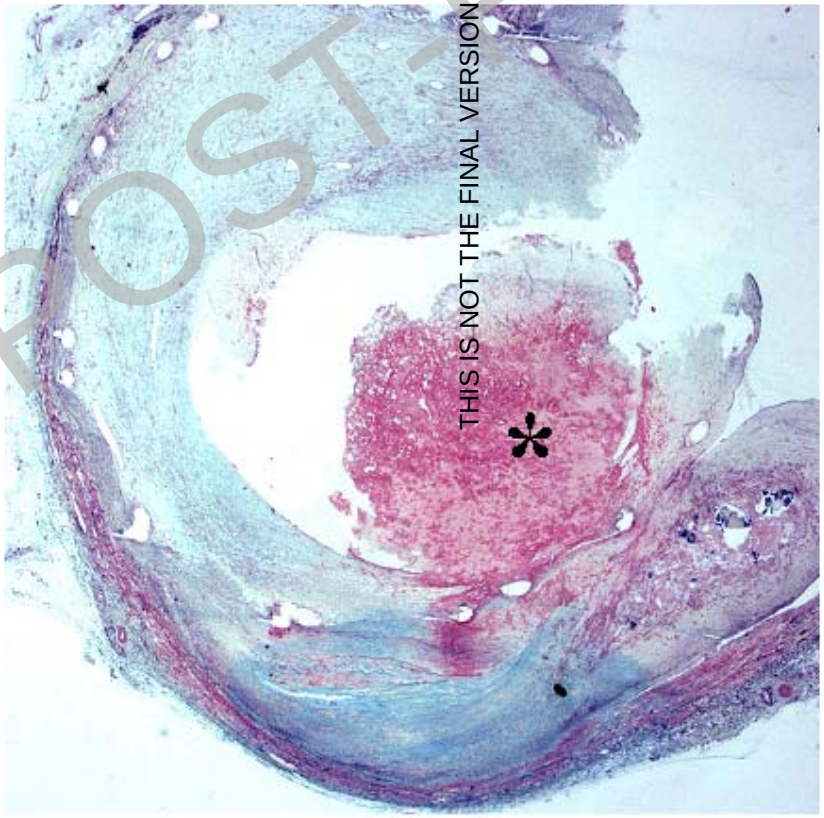

Figure 4

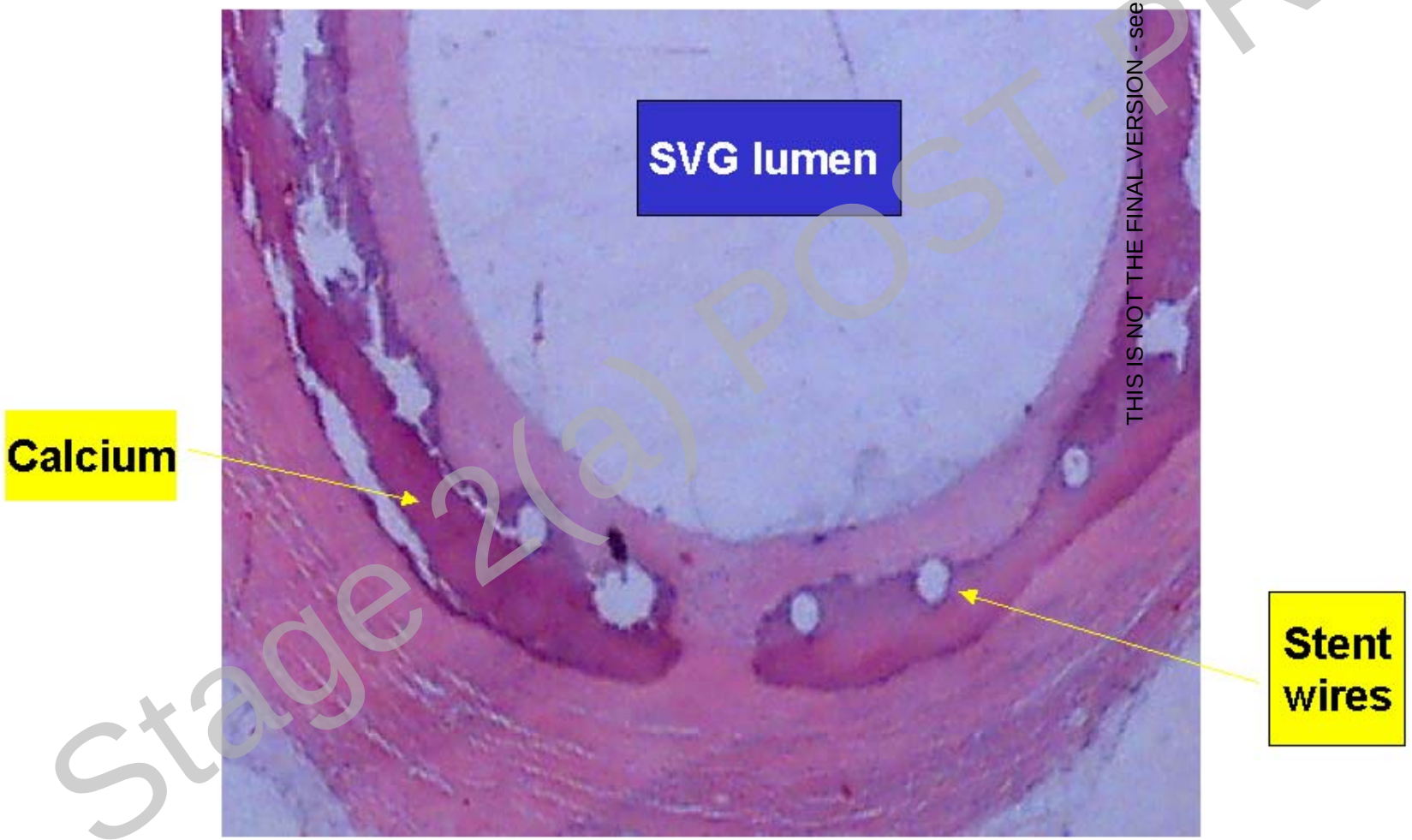

Figure 5

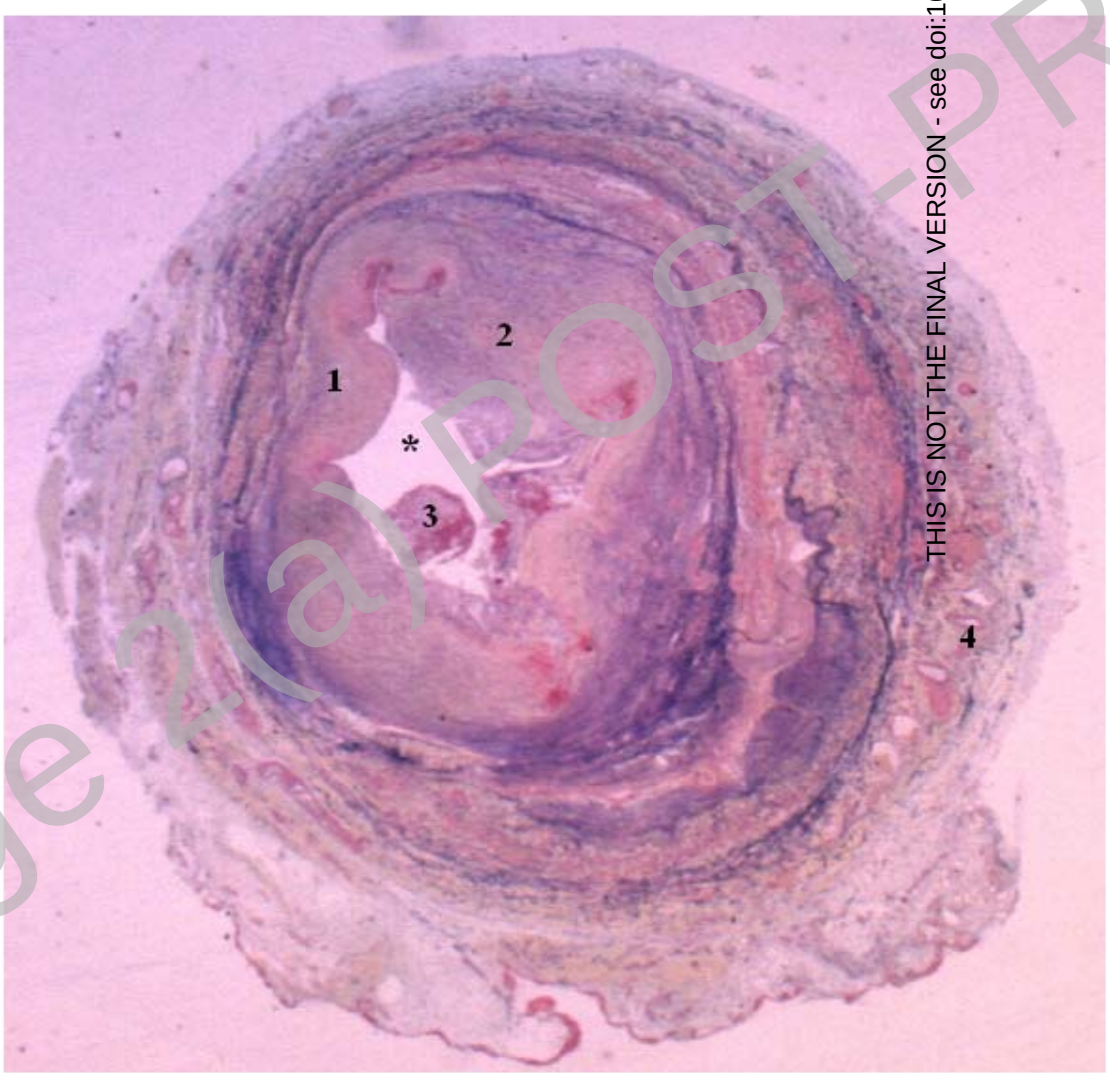

Figure 6

(a)

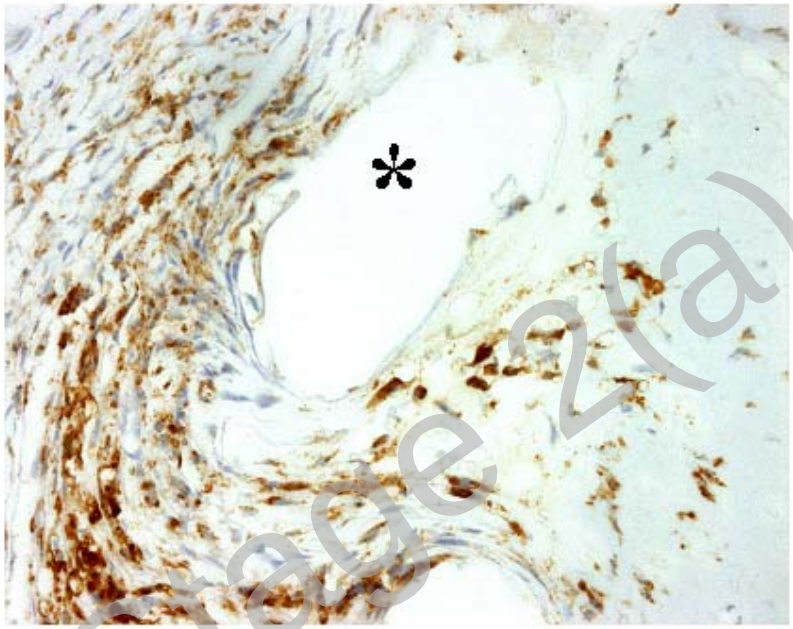

(b)